RESEARCH ARTICLE

Regional Selectivity of Neuromelanin Changes in the Substantia Nigra in Atypical Parkinsonism

Lydia Chougar, MD,[1,2,3*] Emina Arsovic, MD,[2,3,4*] Rahul Gaurav, PhD,[2,3,5] Emma Biondetti, PhD,[2,3,5] Alice Faucher, MD,[6,7] Romain Valabrègue, PhD,[2,5] Nadya Pyatigorskaya, MD, PhD,[2,3,4] Gwendoline Dupont, MD,[8] François-Xavier Lejeune, PhD,[5,9] Florence Cormier, MD, PhD,[5,10] Jean-Christophe Corvol, MD, PhD,[5,11] Marie Vidailhet, MD,[3,5,10] Bertrand Degos, MD, PhD,[6,7] David Grabli, MD, PhD,[5,10] and Stéphane Lehéricy, MD, PhD[2,3,4]

[1]*Sorbonne Université, Institut du Cerveau - Paris Brain Institute - ICM, CNRS, Inria, Inserm, AP-HP, Hôpital de la Pitié Salpêtrière, DMU DIAMENT, Department of Neuroradiology, F-75013, Paris, France, Paris, France*
[2]*ICM, Centre de NeuroImagerie de Recherche–CENIR, Paris, France*
[3]*ICM, Team "Movement Investigations and Therapeutics" (MOV'IT), Paris, France*
[4]*Sorbonne Université, Institut du Cerveau - Paris Brain Institute - ICM, CNRS, Inserm, AP-HP, Hôpital de la Pitié Salpêtrière, DMU DIAMENT, Department of Neuroradiology, F-75013, Paris, France, Paris, France*
[5]*Sorbonne Université, Institut du Cerveau - Paris Brain Institute - ICM, CNRS, Inserm, F-75013, Paris, France*
[6]*Dynamics and Pathophysiology of Neuronal Networks Team, Center for Interdisciplinary Research in Biology, Collège de France, CNRS UMR7241/INSERM U1050, Université PSL, Paris, France*
[7]*Service de Neurologie, Hôpital Avicenne, Hôpitaux Universitaires de Paris Seine-Saint-Denis, APHP, Bobigny, France*
[8]*Centre hospitalier universitaire François Mitterrand, Département de Neurologie, Université de Bourgogne, Dijon, France*
[9]*ICM, Data and Analysis Core, Paris, France*
[10]*Clinique des mouvements anormaux, Département de Neurologie, Assistance Publique Hôpitaux de Paris, Hôpital Pitié-Salpêtrière, Paris, France*
[11]*ICM, Centre d'Investigation Clinique Neurosciences, Paris, France*

ABSTRACT: Background: Neurodegeneration in the substantia nigra pars compacta (SNc) in parkinsonian syndromes may affect the nigral territories differently.
Objective: The objective of this study was to investigate the regional selectivity of neurodegenerative changes in the SNc in patients with Parkinson's disease (PD) and atypical parkinsonism using neuromelanin-sensitive magnetic resonance imaging (MRI).
Methods: A total of 22 healthy controls (HC), 38 patients with PD, 22 patients with progressive supranuclear palsy (PSP), 20 patients with multiple system atrophy (MSA, 13 with the parkinsonian variant, 7 with the cerebellar variant), 7 patients with dementia with Lewy body (DLB), and 4 patients with corticobasal syndrome were analyzed. volume and signal-to-noise ratio (SNR) values of the SNc were derived from neuromelanin-sensitive MRI in the whole SNc. Analysis of signal changes was performed in the sensorimotor, associative, and limbic territories of the SNc.
Results: SNc volume and corrected volume were significantly reduced in PD, PSP, and MSA versus HC. Patients with PSP had lower volume, corrected volume, SNR, and contrast-to-noise ratio than HC and patients with PD and MSA. Patients with PSP had greater SNR reduction in the associative region than HC and patients with PD and MSA. Patients with PD had reduced SNR in the sensorimotor territory, unlike patients with PSP. Patients with MSA did not differ from patients with PD.

***Correspondence to:** Dr. L. Chougar, Centre de NeuroImagerie de Recherche–CENIR, Institut du Cerveau–ICM, Hôpital Pitié-Salpêtrière, 47 Boulevard de l'Hôpital, 75651 Paris Cedex 13, France; E-mail: chougar.lydia@gmail.com

*Co-first authors, equally contributed to the work.

Relevant conflicts of interest/financial disclosures: No relevant conflicts of interest related to the present study.

Funding agencies: This work was supported by grants from Agence Nationale de la Recherche (grant numbers ANR-11-INBS-0006 [France Life Imaging], ANRMNP 2009 [Nucleipark], ANR-11-INBS-0011 [NeurATRIS, Investissements d'Avenir], ANR-19-P3IA-0001 [PRAIRIE 3IA Institute], and ANR-10-IAIHU-06 [IHU–Paris Institute of Neurosciences]), Association France Parkinson, Ecole Neuroscience de Paris, Électricité de France (Fondation d'Entreprise EDF), Institut National de la Santé et de la Recherche Médicale, DHOS-Inserm (2010, Nucleipark), PSP France, and the Fondation Thérèse and René Planiol pour l'étude du Cerveau. Lydia Chougar is supported by an Inria/AP-HP "Poste d'accueil.

[Correction added on 19 April 2022, after first online publication: The correspondence email address has been updated and the co-first author footnote has been added.]

Received: 1 November 2021; **Revised:** 15 February 2022; **Accepted:** 17 February 2022

Published online 29 March 2022 in Wiley Online Library (wileyonlinelibrary.com). DOI: 10.1002/mds.28988

Conclusions: This study provides the first MRI comparison of the topography of neuromelanin changes in parkinsonism. The spatial pattern of changes differed between PSP and synucleinopathies. These nigral topographical differences are consistent with the topography of the extranigral involvement in parkinsonian syndromes.

Key Words: Parkinson's disease; progressive supranuclear palsy; multiple system atrophy; substantia nigra degeneration; neuromelanin-sensitive imaging

Parkinsonism is clinically defined by the association of bradykinesia, plastic rigidity, and asymmetrical resting tremor. Parkinson's disease (PD) is the most common neurodegenerative cause of parkinsonism. Atypical parkinsonism includes tauopathies (progressive supranuclear palsy [PSP] and corticobasal degeneration) and synucleinopathies (multiple system atrophy [MSA] with its cerebellar [MSAc] and parkinsonian [MSAp] subtypes and dementia with Lewy body [DLB]).[1-3]

The hallmark of neurodegenerative parkinsonism is the neurodegeneration of dopaminergic neurons in the substantia nigra pars compacta (SNc).[1-4] Degeneration of dopaminergic neurons has been studied in PD and atypical parkinsonism using neuromelanin-sensitive magnetic resonance imaging (MRI). Neuromelanin is a pigment contained in the dopaminergic neurons that has paramagnetic T1-shortening effects when bound to metals. Volume and signal intensity using neuromelanin-sensitive MRI have been used as surrogate markers for degeneration of dopaminergic neurons in the SNc.[5,6] Reduced SNc neuromelanin volume and signal were reported in PD, PSP, MSA, and corticobasal syndrome (CBS) with high diagnostic accuracy versus healthy controls (HC). Although all studies showed significant changes in PD and atypical parkinsonism, the differences reported between the different types of parkinsonian syndromes were sometimes discordant. Some studies evidenced greater reductions in SNc neuromelanin volume in PSP versus PD, whereas one study reported no significant change in the SNc signal in PSP versus PD and MSA or no significant difference in SNc volume or signal between PD, PSP, and MSA. Similar changes were found between MSA and PD whereas others have reported lower changes in MSAp versus PD.

Disagreement between studies may be attributed to differences in patient characteristics and methodology. Previous studies have also suggested a differential topography of the SNc involvement between diseases. Histological studies have demonstrated a regional selectivity of the dopaminergic neuronal loss in PD. Indeed, the greatest depletion of dopaminergic neurons was shown to occur first in the posterolateral part of the SNc, in the so-called nigrosome 1, before spreading to other nigrosomes and the matrix along rostral, medial, and dorsal axes of progression.[19] This pattern has been recently confirmed using neuromelanin-sensitive MRI.[10] Histological studies have shown that this pattern was similar to MSA but differed from PSP and from aging where the lateral ventral tier was relatively spared.[4]

Here, we investigated the topography of neurodegenerative SNc involvement in patients with PD and atypical parkinsonism in comparison with HC using neuromelanin-sensitive MRI. We assessed changes in signal intensity and volume, identified the different spatial patterns of neurodegeneration in the SNc, and quantified degenerative changes in the motor, associative, and limbic territories of the SNc.

Methods

Population

Participants were prospectively enrolled between April 2017 and June 2020 in the movement disorders clinic of the Pitié-Salpêtrière University Hospital, Paris. The study population included parkinsonian patients with a diagnosis of PD,[20] PSP,[21] MSA,[22] DLB,[23] and CBS[24] established by an expert in movement disorders according to the international diagnostic criteria. Moreover, the clinical diagnosis had to be in agreement with the MRI pattern: (1) for PSP, midbrain atrophy with hummingbird sign,[25] midbrain to pons sagittal area ratio <0.21,[26] or Magnetic resonance parkinsonism index (MRPI) >13.6[27]; (2) for MSAp, posterior putamen atrophy with flattening of the lateral border or increased diffusivity and iron load[28]; (3) for MSAc, pons and cerebellar atrophy with a hot cross bun sign[29]; (4) for CBS, asymmetrical parietocentral atrophy; and (5) no such changes and a third ventricle/internal skull diameter ratio <5.88 in PD.[30]

We recruited age-matched and sex-matched HC with patients without any history of neurological or psychiatric disease. Participants were excluded if they had additional neurological disorders, including stroke or brain tumor on MRI examinations or when the MRI pattern was inconsistent with the clinical diagnosis (eg, MRI typical of MSA in a patient with a clinical diagnosis of PSP or vice versa). The local institutional review board approved the study (Parkatypique: comité de protection des personnes (CPP) Ile-de-France VI08012015). We obtained written informed consent from all participants.

The clinical examination included the Unified Parkinson's Disease Rating Scale Part III scores (UPDRS III) performed in a variable *on* state during the

routine clinical examination with a delay between the MRI and the clinical evaluation ranging from 0 to 94 days (mean ± standard deviation, 26 ± 33 days).

Image Acquisition

Participants were scanned in clinical conditions for diagnostic purposes at the hospital's neuroradiology department using a 3 T SKYRA scanner (Siemens, Erlangen, Germany) with a 64-channel head coil. The MRI protocol included (1) high-resolution three-dimensional T1-weighted gradient-recalled echo sequence (magnetization-prepared rapid acquisition with gradient-recalled echo) with 1-mm isovoxel size and (2) two-dimensional turbo spin echo neuromelanin-sensitive T_1-weighted imaging (repetition time/echo time/flip angle = 890 milliseconds/13 milliseconds/180°, five averages; voxel size, 0.4 × 0.4 × 3 mm^3).

Overall, 13 scans were not analyzed: six as a result of motion artefacts and five because of the presence of exclusion criteria (three patients with MSA and one patient with PSP with normal MRI, one patient with PSP with MRI typical of MSA) and two patients with PD because of misregistration issues.

Analyses in Native Space Based on Manual Segmentations

Data Processing and Segmentation

All analyses were performed using MATLAB (version R2017b; MathWorks Inc, Natick, MA), Statistical Parametric Mapping (SPM12, UK, v7771), FreeSurfer (version 5.3.0; MGH), and FSL (version 5.0; FMRIB, UK). Using FreeSurfer viewer, similar to a previous study,[9] SN_c contours of the left and right SN were manually delineated on neuromelanin-sensitive images by one examiner (E.A.) as the border of hyperintense area dorsal to the cerebral peduncle and ventral to the red nucleus. Contours were continuous as they did not include noncontiguous voxels. The examiner was blind to the clinical status. A background region including the tegmentum and superior cerebral peduncles was also traced.

Volume and Signal Analyses

Volumes of each neuromelanin-based regions of interest (ROIs) were calculated as the product between the voxel size and the number of voxels in the ROIs of the three lowest contiguous image slices where the SN was visible. Total intracranial volume (TIV) was used to correct for variations in individual head size. White matter, gray matter, and cerebrospinal fluid volumes were summed up to provide an estimate of TIV using SPM12. Hence, we calculated corrected volume by dividing SN volumes by TIV to normalize for respective head sizes of the participants. For each slice, the signal-to-noise ratio (SNR) and contrast-to-noise ratio (CNR) were calculated by normalizing the mean signal in SN relative to the background signal using the following formulas:

$$\mathrm{SNR} = \mathrm{mean\_over\_slices}\{(\mathrm{Sig_{SN}}/\mathrm{Sig_{BND}}) \times 100)\}$$

$$\mathrm{CNR} = \mathrm{mean\_over\_slices}\{(\mathrm{Sig_{SN}} - \mathrm{Sig_{BND}})/\mathrm{STD_{BND}}\}$$

where Sig_{SN} is the signal intensity in SNc ROI, Sig_{BND} the signal intensity in background ROI, and STD_{BND} is the standard deviation in background ROI.

For SN volumes and signal intensity, we used the mean values of the left and right SN.

Intraexaminer reproducibility for the segmentations was evaluated using the DICE (Sørensen-Dice) similarity coefficient on a sample of 51 participants.

Analyses in Template Space

To enable anatomical alignment of all SN segmentations, we used a template of the average brain that was calculated in a previous study to be equally representative of HC and patients with prodromal and clinical parkinsonism.[10]

For each participant, the neuromelanin-sensitive image was aligned to the brain template using NiftyReg.[31,32] First, the neuromelanin-sensitive image was rigidly aligned to the corresponding T1-weighted image. Second, the T1-weighted image was aligned to the template using a concatenation of one affine and on nonlinear transformation. The resulting T1-to-template transformation was applied to the neuromelanin-sensitive image with nearest-neighbor interpolation[10,33] (Supplementary Fig. S1).

An analysis was then performed based on the calculation of the neuromelanin SNR in the SNc and its subregions in template space. An SNc mask and a background mask that were previously calculated in template space based on the neuromelanin-sensitive MRIs of 61 HC were used.[10,33] The SNc mask was manually segmented into three regions based on the functional subdivision of the SN in a posterolateral sensorimotor, anteromedial associative, and posteromedial limbic regions.[33,34] These masks were applied to each participant's neuromelanin-sensitive image previously aligned to the brain template. Then, signal values in the whole SNc, in each SNc subregion, and in the background masks were extracted, and the mean SNR values of both sides of the SNc were calculated for each participant (Fig. S2). The codes used for the analyses are available at https://github.com/emmabiondetti/substantia-nigra-neuromelanin.

Of note, analyses in native space and template space studied the SNR in two different and complementary ways: in the remaining less affected SNc and in the

entire SNc using the mask of healthy participants, respectively.

Statistical Analyses

Statistical analyses were performed using R (R Core Team 2019, v3.6.1) R Foundation for Statistical Computing, Vienna, Austria). Clinical and demographic data were compared between groups using the Kruskal–Wallis test followed by pairwise Dunn's tests with Bonferroni correction or Fisher's exact test.

Sex and age were included as covariates of no interest as both sex and age influence the phenotypical expression of PD,[35] and neuromelanin accumulates in the SN with healthy ageing[36,37] influences neuromelanin accumulation. Patients with MSA were analyzed together, and patients with DLB and CBS were excluded from the main analyses given the low number of participants in each group. Exploratory pairwise analyses were subsequently performed to compare HC to patients with DLB, CBS, MSAp, and MSAc on one hand and patients with MSAp to MSAc on the other hand.

Between-group differences in volume, corrected volume, SNR, and CNR were evaluated by fitting general linear models (one model per type of measurement) including group (HC and parkinsonian groups) as the only between-group factor, with age and sex for covariate adjustment. Based on the fitted generalized linear models, the group difference was tested by type II analysis of variance (ANOVA) *F* test. If a significant difference was found, post hoc pairwise comparisons were conducted by using Tukey's method in the emmeans package.

For measurements in template space, the data were first analyzed using the same procedure as before to test for between-group differences in SNR values in the whole SNc. Then, a second analysis was performed to investigate the spatial pattern of dopaminergic neuron loss in the SN in parkinsonian syndromes. SNR values in the sensorimotor, associative, and limbic territories were compared through linear mixed-effect models (LMMs; one model per parameter of interest). In these models, group, region, and their interaction terms were regarded as fixed effects, whereas the participant identifier was assigned as a random effect (intercept) to account for the repeated measurements acquired in the different ROIs for the same participant. Age and sex were also included for covariate adjustments. All LMMs were fitted using restricted maximum-likelihood estimation from the function lmer in the lme4 package. Significance for the main effects and the two-way interaction of group and region were assessed based on type II Wald chi-square tests using the function ANOVA in the car package. Post hoc pairwise comparisons were performed on a significant interaction or main factor effect with the emmeans package to further determine where the differences occurred across the study groups and the ROIs. All *P* values from the post hoc tests were obtained using Kenward–Roger's approximation for degrees of freedom (*df*) and after adjustment for multiple testing by Tukey's method.

For each model, the assumptions of normality and constant variance of residuals were checked afterward. The level of statistical significance was set at $P < 0.05$ for all tests. Correlations between SNR values and clinical variables were also investigated (see the Supplementary Material).

Results

Participant Characteristics

We included 22 HC, 38 patients with PD, 22 patients with PSP, 13 patients with MSAp, seven patients with MSAc, seven patients with DLB, and four patients with CBS (Table 1). MRI scans were obtained on average within 22.5 ± 26.9 days after the clinical examination. There were no between-group differences in sex proportion ($P = 0.40$). Age was significantly different between groups ($P = 0.001$), with patients with PSP being older than patients with MSAc ($P = 0.02$). UPDRS III scores ($P = 0.11$) and disease duration ($P = 0.21$) did not differ significantly between patient groups.

Group Differences in Neuromelanin Volume and Signal Based on Manual Segmentations

On neuromelanin-sensitive imaging, the signal intensity of the SNc was visually decreased in patients with parkinsonian syndromes in comparison with HC (Fig. S3).

There was a high intrarater reproducibility for manual segmentations (DICE = 0.81).

There was a significant difference in SNc volume ($F = 52.49$, $df = 3$, $P < 0.001$), corrected volume ($F = 44.18$, $df = 3$, $P < 0.001$), SNR ($F = 7.50$, $df = 3$, $P < 0.001$), and CNR ($F = 6.70$, $df = 3$, $P < 0.001$) when comparing all groups. Post hoc comparisons showed that HC had higher SN volume and corrected volume than PD, PSP, and MSA ($P \leq 0.001$) and higher SNR and CNR values than PSP ($P < 0.01$). Patients with PSP had lower volume and corrected volume than patients with PD ($P < 0.01$ and $P < 0.001$, respectively) and MSA ($P < 0.05$), lower SNR values than patients with PD ($P < 0.001$) and MSA ($P < 0.05$), and lower CNR values than patients with PD ($P < 0.001$) with a trend for patients with MSA ($P = 0.05$) (Table 2, Fig. 1). There were no differences between patients with PD and MSA.

The exploratory pairwise comparisons showed higher SN volume and corrected volume in HC versus DLB and CBS ($P < 0.01$ for volume and $P < 0.05$ for corrected volume, respectively) and MSAp and MSAc ($P < 0.0001$). There was no SNR or CNR difference.

TABLE 1 *Clinical characteristics*

Groups	HC	PD	PSP	MSA			DLB	CBS
				Total	MSAp	MSAc		
Participants, n	22	38	22	20	13	7	7	4
Age at MRI, years, mean ± SD	64.7 ± 7.3	66.2 ± 9.8	71.1 ± 7.4	60.8 ± 7.4	62.2 ± 8.7	58.3 ± 7.8	73.7 ± 10.1	76.0 ± 6.7
Sex, male/female, n	12/10	24/14	11/11	12/8	6/7	6/1	6/1	2/2
Disease duration, years, mean ± SD[a]	NA	4.8 ± 3.3	4.7 ± 3.2	3.6 ± 1.3	4.2 ± 1.6	2.4 ± 1.3	3.1 ± 1.5	3.0 ± 2.7
UPDRS III scores, mean ± SD (number of participants with available data)	0.1 ± 0.3	19.6 ± 10.6 (15)	32.0 ± 15.7 (13)	18.9 ± 5.6 (7)	22.5 ± 14.9 (2)	17.4 ± 5.2 (5)	16.0 (1)	NA

Abbreviations: HC, healthy controls; PD, Parkinson's disease; PSP, progressive supranuclear palsy; MSA, multiple system atrophy; MSAp, multiple system atrophy of the parkinsonian type; MSAc, multiple system atrophy of the cerebellar type; DLB, dementia with Lewy body; CBS, corticobasal syndrome; MRI, magnetic resonance imaging; SD, standard deviation; UPDRS III, Unified Parkinson's disease Rating Scale Part III; NA, not applicable.
[a]Disease duration was calculated using the date of first symptoms as the starting point.

TABLE 2 *Neuromelanin measurements in the substantia nigra*

Groups	HC	PD	PSP	MSA	Exploratory analyses			
					MSAp	MSAc	DLB	CBS
Volume, mm^3	307.1 ± 51.0 (b,c,d)	188.3 ± 46.5 (a,c)	144.8 ± 40.3 (a,b,d)	186.7 ± 37.9 (a,c)	198.7 ± 38.8	164.4 ± 25.2	227.3 ± 45.7	206.3 ± 27.4
Corrected volume, mm^3	0.22 ± 0.04 (b,c,d)	0.13 ± 0.04 (a,c)	0.10 ± 0.03 (a,b,d)	0.13 ± 0.03 (a,c)	0.14 ± 0.03	0.11 ± 0.02	0.16 ± 0.03	0.15 ± 0.01
SNR	110.1 ± 1.7 (c)	110.4 ± 1.9 (c)	108.0 ± 2.8 (a,b,d)	109.5 ± 2.3 (c)	109.3 ± 2.0	110.0 ± 2.9	109.3 ± 1.2	110.7 ± 1.2
CNR	1.21 ± 0.21 (c)	1.22 ± 0.24 (c)	0.94 ± 0.40 (a,b,*d*)	1.10 ± 0.30 (*c*)	1.10 ± 0.27	1.10 ± 0.37	1.10 ± 0.25	1.30 ± 0.16

Results are presented as mean ± standard deviation. a–d indicate significant differences versus (a) HC, (b) PD, (c) PSP, and (d) MSA. Letters in italics indicate trends without statistical significance ($0.05 < P \leq 0.1$).
Abbreviations: HC, healthy controls; PD, Parkinson's disease; PSP, progressive supranuclear palsy; MSA, multiple system atrophy; MSAp, multiple system atrophy of the parkinsonian type; MSAc, multiple system atrophy of the cerebellar type; DLB, dementia with Lewy body; CBS, corticobasal syndrome; SNR, signal-to-noise ratio; CNR, contrast-to-noise ratio.

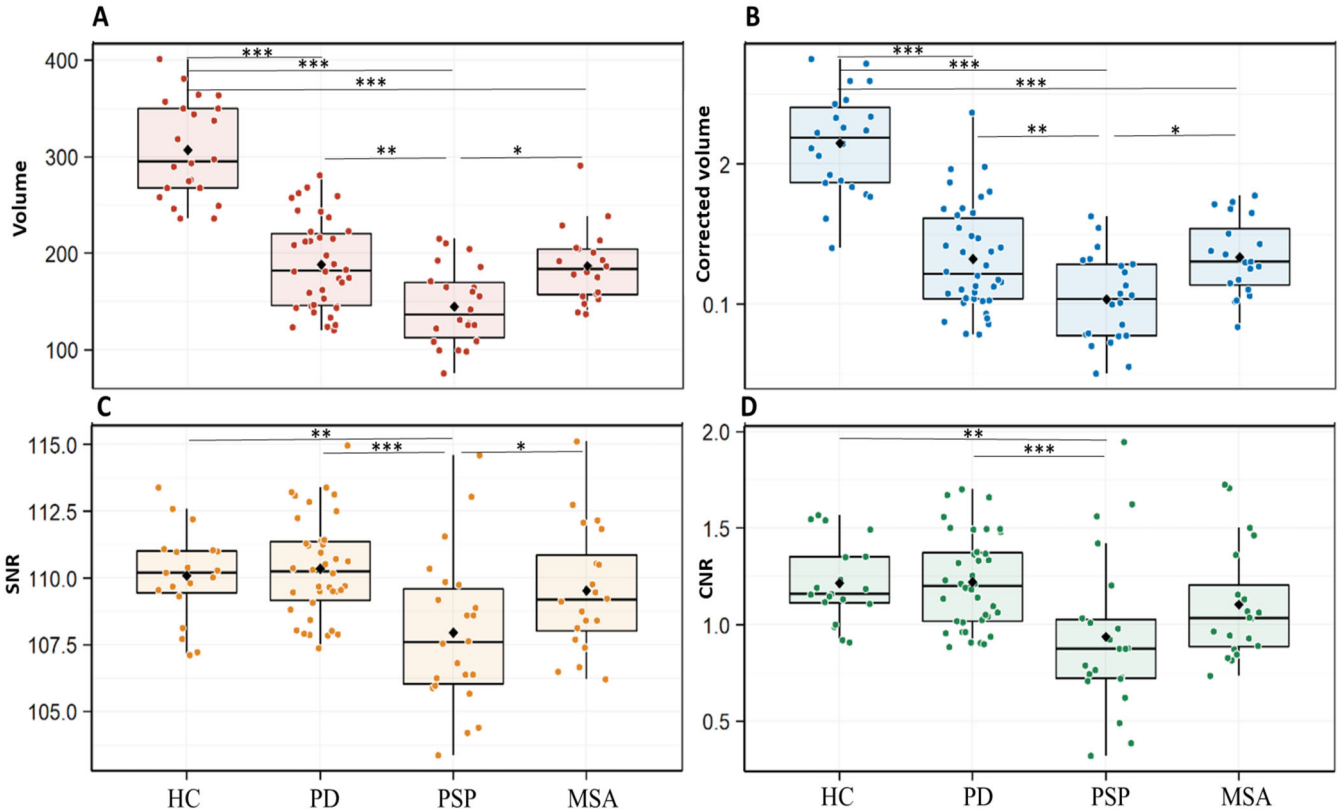

FIG. 1. Between-group comparison of substantia nigra volume (**A**), corrected volume (**B**), SNR (**C**), and CNR (**D**) in participant groups. ***$P < 0.001$; **$0.001 < P \leq 0.01$; *$0.001 < P \leq 0.05$. CNR, contrast-to-noise ratio; HC, healthy control, MSA, multiple system atrophy; PD, Parkinson's disease; PSP, progressive supranuclear palsy; SNR, signal-to-noise ratio. [Color figure can be viewed at wileyonlinelibrary.com]

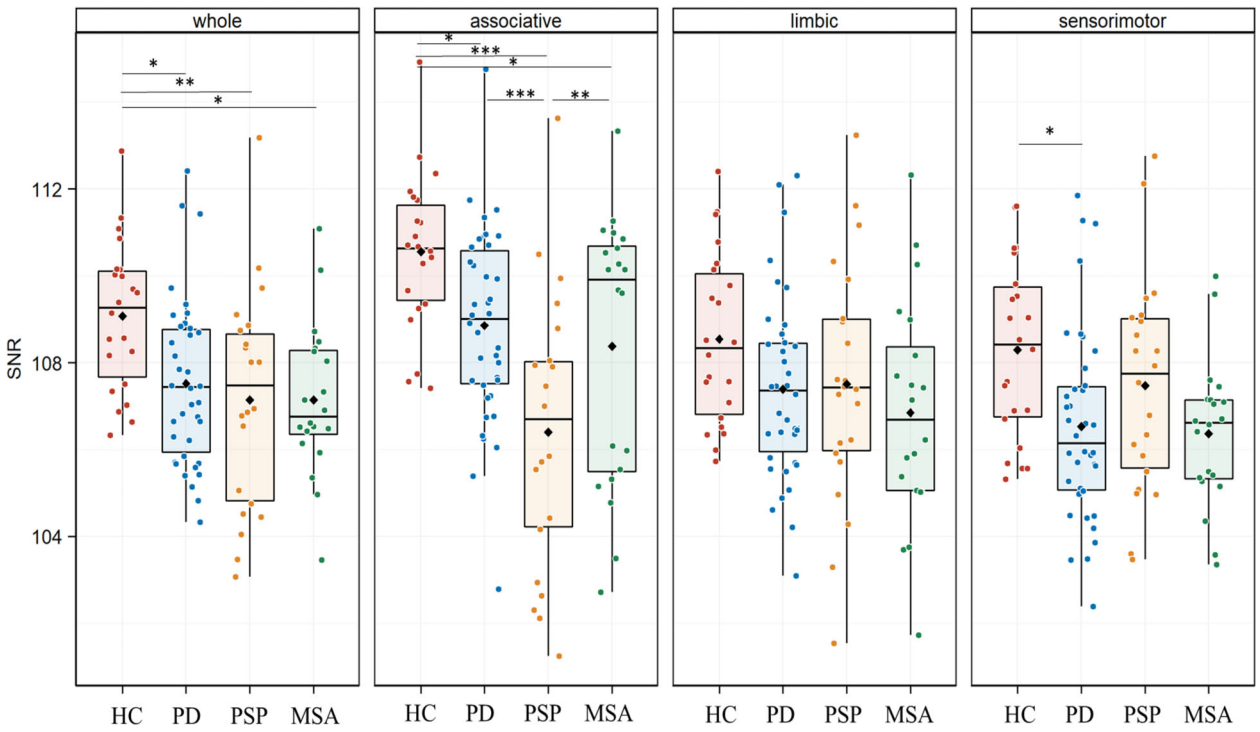

FIG. 2. Between-group comparison of SNR values in the whole substantia nigra and its three territories. ***$P < 0.001$; **$0.001 < P \leq 0.01$; *$0.01 < P \leq 0.05$. HC, healthy control; MSA, multiple system atrophy; PD, Parkinson's disease; PSP, progressive supranuclear palsy with Richardson syndrome; SNR, signal-to-noise ratio. [Color figure can be viewed at wileyonlinelibrary.com]

MSAp had higher SN volume than MSAc ($P < 0.05$), without any difference in corrected volume, SNR, or CNR.

Spatial Distribution of Neuromelanin Changes

Analyses performed in the mask of the whole SNc in template space confirmed that SNR values were significantly different between groups (type II ANOVA, $F = 5.20$, $df = 3$, $P = 0.002$). Post hoc comparisons indicated lower values in patients with PD ($P = 0.016$), PSP ($P = 0.002$), and MSA ($P = 0.02$) versus HC without differences between patient groups (Fig. 2, Supplementary Table 1).

When comparing the three SN territories between groups, there was a significant effect of the group ($\chi^2 = 16.01$, $df = 3$, $P = 0.001$) and region ($\chi^2 = 51.90$, $df = 2$, $P < 0.0001$) factors with a significant group by region interaction ($\chi^2 = 47.02$, $df = 6$, $P < 0.0001$). Post hoc comparisons showed that SNR values in the associative territory were lower in patients with PSP ($P < 0.0001$), PD ($P = 0.04$), and MSA ($P = 0.03$) than in HC and lower in patients with PSP versus patients with PD ($P < 0.0001$) and MSA ($P = 0.01$). In the sensorimotor territory, SNR values were lower in PD than in HC ($P = 0.03$) and also lower in patients with MSA than in HC, but the difference did not reach significance ($P = 0.08$). There were no significant differences in the limbic territory or between PD and MSA (Figs. 2 and 3, Supplementary Table 1).

Exploratory pairwise comparisons showed that SNR values in the whole SN were lower in DLB ($P = 0.01$) and MSAp ($P = 0.001$) in comparison with HC, with

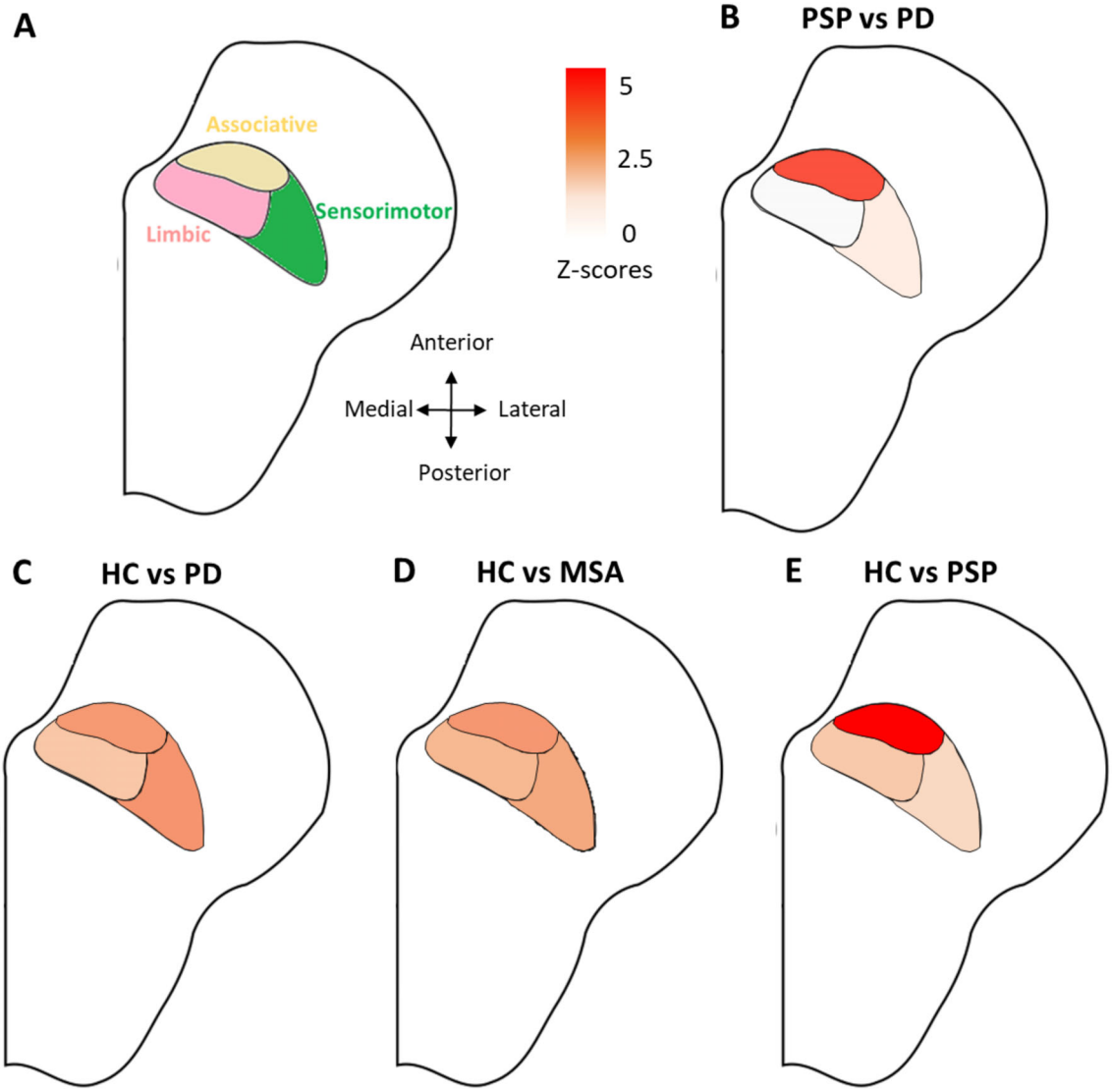

FIG. 3. (A) Location of the functional territories in the substantia nigra. Results of the statistical comparisons between (B) patients with PD and PSP, (C) HC and patients with PD, (D) HC and patients with MSA, and (E) HC and patients with PSP. Results were adjusted for age and sex, and p-values were corrected for multiple comparisons by Tukey's method. Statistical significance was set to a corrected p<0.05. For improved clarity in the visual representation of statistical differences, p-values were converted into Z-scores. Color-coding indicates z-scores levels.

an involvement of the associative ($P = 0.002$) and sensorimotor ($P = 0.02$) territories in DLB, and all territories in MSAp (associative, $P = 0.004$; limbic, $P = 0.04$; sensorimotor, $P = 0.006$). No difference was seen between HC and CBS, HC and MSAc, or MSAp and MSAc.

When comparing SNR values between the three territories within each group, in HC and patients with PD and MSA, the associative territory had significantly higher SNR values than the limbic and sensorimotor territories (Fig. S4). In PD but not in HC or MSA, the sensorimotor territory also had a significantly lower SNR value than the limbic territory. In contrast, in patients with PSP, this pattern was reversed with the associative territory having lower SNR values than the limbic and sensorimotor territories.

For all models, a visual inspection of the residual distributions did not show any important deviation from the normality and variance–variance assumptions.

Discussion

This study provides the first MRI comparison of the topography of neuromelanin changes in parkinsonism. We confirm that neuromelanin volume and signal were reduced in parkinsonian disorders. The spatial pattern of changes differed between PSP and synucleinopathies. Compared with other groups, PSP had greater changes in the associative region. SNR in the sensorimotor territory was preserved in PSP, but reduced in PD, and there was a trend in MSA. There was no significant difference between MSA and PD. Exploratory analyses showed reduced SN volumes in the DLB and CBS groups and no differences between MSAp and MSAc.

SN Anatomy

The anatomy of the SN is complex, involving several distinct compartments with different afferent and efferent projections. Human histological studies have parcellated the SN into three oblique bands including the dorsal tier of pars compacta, which corresponded to the upper and posterior part of the SNc; the ventral tier of pars compacta, corresponding to the lower and anterior part of the SNc; and the pars reticulata, located anteriorly to the SNc.[4] These SN regions have distinct connections to the striosome and matrix compartments of the striatum[38] and to the sensorimotor (lateral SN), associative (central SN), and limbic (medial SN) striatal regions.[39] Using diffusion-based tractography in humans, these regions were shown to be connected to the sensorimotor cortex (dorsolateral SNc), the frontal cortex and insula (ventral SNc), and limbic areas including the lateral and medial orbitofrontal cortex, hippocampus, and amygdala (dorsomedial SNc).[34] A better description of the topographical differences in the involvement of the SN in parkinsonian syndromes could thus allow a better understanding of their pathophysiology.

Regional Selectivity of Neuromelanin Changes

In PD, degeneration predominated in the posterolateral part of the caudal SN as shown in histological[4,19,40,41] and MRI studies.[10,33] This region corresponded to the lateral ventral tier of the SN[4] and to the sensorimotor territory of the SNc.[10] It was shown to project to the sensorimotor striatum in primates,[42] corresponding to the posterior sensorimotor territory of the putamen, the area of greatest dopaminergic denervation in patients with PD.[10,43] Changes in this nigral region correlated with the severity of motor symptoms in PD as demonstrated using neuromelanin imaging[9,10,15,16] or diffusion imaging.[44,45] In our study, the associative territory was also involved in patients with PD. Histological studies showed that in PD, the regional neuronal loss started in the ventrolateral sensorimotor territory and then spread to the ventromedial associative territory.[4] A recent study using neuromelanin imaging reported similar spatial and temporal gradients in the SNc involving first the sensorimotor and then the associative and limbic regions.[33]

In patients with MSA, the neuromelanin signal was decreased in the associative territory with a trend in the sensorimotor territory compared with HC. There was no significant difference between MSA and PD. Histology studies reported variable results. In MSAp, formerly known as striatonigral degeneration, the pattern of cell loss has been variously described as affecting the lateral and medial,[46] lateral and caudal,[47] lateral and midportion,[48] dorsolateral,[49] and ventral and middle parts of the SNc.[50] Lateral predominance therefore seemed to be reported by many authors. The absence of difference between MSA and PD is also in agreement with previous histological studies in which the distribution of pigmented neuron loss in MSA estimated by neuronal counting was similar to that of PD[4] and with neuromelanin-based MRI studies, which found no difference between MSA and PD.[13,17] In MSA, although a predominant involvement of the sensorimotor posterolateral putamen was reported in histological,[49,51] MRI,[52-54] ^{18}F-fluorodeoxyglucose,[55] and ^{18}F-dopa positron emission tomography studies[56] and presynaptic dopamine transporter single-photon emission tomography studies,[57] hypometabolism[56] and reduction in dopaminergic function[57] are also observed in the anterior striatum in line with the involvement of the associative SN observed in our study.

Patients with PSP had lower SNc volume and SNR than other groups using manual ROI, with greater involvement of the associative territory. These findings are consistent with those from a previous study using free-water imaging that showed higher free-water values in PSP compared with other groups. However,

although both the anterior and posterior SN were affected in that study, only the anterior portion, partly including the associative territory, was significantly involved here.[58] Our results were also in agreement with a histological study that did not find elective involvement of the lateral ventral region of the SN, the region most affected in PD, but greater cell loss in the ventromedial SN.[4] In monkeys, using retrograde transport of horseradish peroxidase, the dorsolateral frontal cortex was connected to the more anterior portions in the medial one-half and dorsal-most part of the SNc.[59] In humans, the ventral SNc was preferentially connected with the prefrontal cortex, anterior cingulate cortex, and anterior insula.[34] In patients with PSP, these frontal regions are particularly affected as shown using positron emission tomography with ^{18}F-fluorodeoxyglucose[55] and flortaucipir tau tracer as well as MRI structural and diffusion imaging.[60] In many neurodegenerative disorders such as PD[61,62] and Alzheimer's disease,[63,64] neuropathological changes follow a stereotyped regional pattern of progression over time. Changes are greater in brain regions that are densely connected, probably as a result of the transneuronal spread of the disease process.[65,66] Imaging studies also provided support to this mechanism of transmission.[67] In PSP, early histological lesions were most prominent in the midbrain and deep brain nuclei and spread to the cortical regions in advanced stages of the disease.[68] Our results are in agreement with the hypothesis that the greatest changes in the neuromelanin signal should be observed in the SN region connected to the frontal cortical areas most affected in PSP.

In patients with DLB, exploratory analyses showed reduced neuromelanin signal in the whole SNc and in the associative and sensorimotor territories. Histological[69,70] and MRI studies[6,16] showed a decrease in dopaminergic neurons density and the neuromelanin signal in DLB. Previous histological studies reported an overlap in the pattern of neuropathological changes between PD and DLB.[69,70]

In patients with CBS, there was a decrease in SN volume in line with previous findings, but not in signal using the template-based approach. This was probably due to a lack of statistical power.

Limitations

There were some limitations to this work. Some patient groups included only a few patients, which may have masked differences because of a lack of statistical power. There was no histological confirmation of the diagnosis of parkinsonism, which was based on international clinical criteria. However, we took care to ensure the diagnoses by adding an imaging inclusion criterion characteristic of each pathology, which limited the risk of participants being misclassified. Patients with PSP were older than patients with MSAc. To take into account the potential effect of age in the analyses, age was used as a covariate. Assessment of UPDRS III scores was performed in a variable *on* state during the routine clinical examination, with a variable delay between MRI and clinical examination, and a number of values were missing, which limited correlation analyses. Furthermore, we used the average values on both sides of the SNc because information on which side was clinically more or less affected was missing for many participants. Therefore, the possible asymmetry of the SNc degeneration was not investigated. We used manual segmentation to delineate the SN, which allows careful quality control of images with good reproducibility in previous studies.[9,10] However, automated or semiautomated segmentation could be faster and more reproducible.[71-73] Regarding the registration procedure, some degree of misalignment may occur between neuromelanin-sensitive images and the template. However, we took several measures to mitigate this effect.

Conclusion

Spatial patterns of SNc degeneration differed between PD and PSP, but not between synucleinopathies (PD and MSA). In future studies, multimodal neuroimaging analysis of the involvement of the SNc territories, the striatum, and the cortex could help identify the networks affected in parkinsonian syndromes. Furthermore, longitudinal studies in larger populations are needed to confirm these findings and could allow determining the progression of neuromelanin changes over time.

Data Availability Statement

The data that support the findings of this study are available on request from the corresponding author. The data are not publicly available due to privacy or ethical restrictions.

References

1. Dickson DW. Parkinson's disease and parkinsonism: neuropathology. Cold Spring Harb Perspect Med 2012;2:a009258.
2. Dickson DW. Neuropathology of Parkinson disease. Parkinsonism Relat Disord 2018;46((suppl 1)):S30–S33.
3. Levin J, Kurz A, Arzberger T, Giese A, Höglinger GU. The differential diagnosis and treatment of atypical parkinsonism. Dtsch Arzteblatt Int 2016;113:61–69.
4. Fearnley JM, Lees AJ. Ageing and Parkinson's disease: substantia nigra regional selectivity. Brain J Neurol 1991;114(Pt 5)):2283–2301.
5. Cassidy CM, Zucca FA, Girgis RR, et al. Neuromelanin-sensitive MRI as a noninvasive proxy measure of dopamine function in the human brain. Proc Natl Acad Sci U S A 2019;116:5108–5117.

6. Kitao S, Matsusue E, Fujii S, et al. Correlation between pathology and neuromelanin MR imaging in Parkinson's disease and dementia with Lewy bodies. Neuroradiology 2013;55:947–953.
7. Pyatigorskaya N, Gaurav R, Arnaldi D, et al. Magnetic resonance imaging biomarkers to assess substantia Nigra damage in idiopathic rapid eye movement sleep behavior disorder. Sleep 2017;40. https://doi.org/10.1093/sleep/zsx149
8. Sasaki M, Shibata E, Tohyama K, et al. Neuromelanin magnetic resonance imaging of locus ceruleus and substantia nigra in Parkinson's disease. Neuroreport 2006;17:1215–1218.
9. Gaurav R, Yahia-Cherif L, Pyatigorskaya N, et al. Longitudinal changes in Neuromelanin MRI signal in Parkinson's disease: a progression marker. Mov Disord 2021;36(7):1592–1602.
10. Biondetti E, Gaurav R, Yahia-Cherif L, et al. Spatiotemporal changes in substantia nigra neuromelanin content in Parkinson's disease. Brain 2020;143(9):2757–2770.
11. Cho SJ, Bae YJ, Kim J-M, et al. Diagnostic performance of neuromelanin-sensitive magnetic resonance imaging for patients with Parkinson's disease and factor analysis for its heterogeneity: a systematic review and meta-analysis. Eur Radiol 2021;31:1268–1280.
12. Kashihara K, Shinya T, Higaki F. Reduction of neuromelanin-positive nigral volume in patients with MSA, PSP and CBD. Intern Med 2011;50:1683–1687.
13. Ohtsuka C, Sasaki M, Konno K, et al. Differentiation of early-stage parkinsonisms using neuromelanin-sensitive magnetic resonance imaging. Parkinsonism Relat Disord 2014;20:755–760.
14. Pyatigorskaya N, Yahia-Cherif L, Gaurav R, et al. Multimodal magnetic resonance imaging quantification of brain changes in progressive supranuclear palsy. Mov Disord 2020;35:161–170.
15. Taniguchi D, Hatano T, Kamagata K, et al. Neuromelanin imaging and midbrain volumetry in progressive supranuclear palsy and Parkinson's disease: Neuromelanin-MRI and midbrain Volumetry. Mov Disord 2018;33:1488–1492.
16. Matsuura K, Ii Y, Maeda M, et al. Neuromelanin-sensitive magnetic resonance imaging in disease differentiation for parkinsonism or neurodegenerative disease affecting the basal ganglia. Parkinsonism Relat Disord 2021;87:75–81.
17. Matsuura K, Maeda M, Yata K, et al. Neuromelanin magnetic resonance imaging in Parkinson's disease and multiple system atrophy. Eur Neurol 2013;70:70–77.
18. Simões RM, Castro Caldas A, Grilo J, et al. A distinct neuromelanin magnetic resonance imaging pattern in parkinsonian multiple system atrophy. BMC Neurol 2020;20:432
19. Damier P, Hirsch EC, Agid Y, Graybiel AM. The substantia nigra of the human brain. I. Nigrosomes and the nigral matrix, a compartmental organization based on calbindin D(28K) immunohistochemistry. Brain. J Neurol 1999;122(Pt 8):1421–1436.
20. Postuma RB, Berg D, Stern M, et al. MDS clinical diagnostic criteria for Parkinson's disease. Mov Disord 2015;30:1591–1601.
21. Höglinger GU, Respondek G, Stamelou M, et al. Clinical diagnosis of progressive supranuclear palsy: the movement disorder society criteria. Mov Disord 2017;32:853–864.
22. Gilman S, Wenning GK, Low PA, et al. Second consensus statement on the diagnosis of multiple system atrophy. Neurology 2008;71:670–676.
23. McKeith IG, Boeve BF, Dickson DW, et al. Diagnosis and management of dementia with Lewy bodies. Neurology 2017;89:88–100.
24. Armstrong MJ, Litvan I, Lang AE, et al. Criteria for the diagnosis of corticobasal degeneration. Neurology 2013;80:496–503.
25. Mueller C, Hussl A, Krismer F, et al. The diagnostic accuracy of the hummingbird and morning glory sign in patients with neurodegenerative parkinsonism. Parkinsonism Relat Disord 2018;54:90–94.
26. Möller L, Kassubek J, Südmeyer M, et al. Manual MRI morphometry in parkinsonian syndromes. Mov Disord 2017;32:778–782.
27. Quattrone A, Nicoletti G, Messina D, et al. MR imaging index for differentiation of progressive supranuclear palsy from Parkinson disease and the Parkinson variant of multiple system atrophy. Radiology 2008;246:214–221.
28. Bajaj S, Krismer F, Palma J-A, et al. Diffusion-weighted MRI distinguishes Parkinson disease from the parkinsonian variant of multiple system atrophy: a systematic review and meta-analysis. PloS One 2017;12:e0189897
29. Watanabe H, Saito Y, Terao S, et al. Progression and prognosis in multiple system atrophy: an analysis of 230 Japanese patients. Brain J Neurol 2002;125:1070–1083.
30. Quattrone A, Antonini A, Vaillancourt DE, et al. A new MRI measure to early differentiate progressive Supranuclear palsy from De novo Parkinson's disease in clinical practice: an international study. Mov Disord 2021;36:681–689.
31. Ourselin S, Roche A, Subsol G, Pennec X, Ayache N. Reconstructing a 3D structure from serial histological sections. Image Vis Comput 2001;19:25–31.
32. Modat M, Ridgway GR, Taylor ZA, et al. Fast free-form deformation using graphics processing units. Comput Methods Programs Biomed 2010;98:278–284.
33. Biondetti E, Santin MD, Valabrègue R, et al. The spatiotemporal changes in dopamine, neuromelanin and iron characterizing Parkinson's disease. Brain 2021;144(10):3114–3125.
34. Zhang Y, Larcher KM, Misic B, Dagher A. Anatomical and functional organization of the human substantia nigra and its connections. eLife 2017;6:e26653.
35. Prange S, Danaila T, Laurencin C, et al. Age and time course of long-term motor and nonmotor complications in Parkinson disease. Neurology 2019;92:e148–e160.
36. Zecca L, Stroppolo A, Gatti A, et al. The role of iron and copper molecules in the neuronal vulnerability of locus coeruleus and substantia nigra during aging. Proc Natl Acad Sci U S A 2004;101:9843–9848.
37. Xing Y, Sapuan A, Dineen RA, Auer DP. Life span pigmentation changes of the substantia nigra detected by neuromelanin-sensitive MRI. Mov Disord 2018;33:1792–1799.
38. Gerfen CR, Herkenham M, Thibault J. The neostriatal mosaic: II. Patch- and matrix-directed Mesostriatal dopaminergic and non-dopaminergic systems. J Neurosci 1987;7(12):3915–3934.
39. Haber SN. The place of dopamine in the cortico-basal ganglia circuit. Neuroscience 2014;282:248–257.
40. Hirsch E, Graybiel AM, Agid YA. Melanized dopaminergic neurons are differentially susceptible to degeneration in Parkinson's disease. Nature 1988;334:345–348.
41. Jellinger K, Danielczyk W. Striato-nigrale degeneration. Acta Neuropathol 1968;10(3):242–257. https://doi.org/10.1007/BF00687726
42. Haber SN. The primate basal ganglia: parallel and integrative networks. J Chem Neuroanat 2003;26:317–330.
43. Kish SJ, Shannak K, Hornykiewicz O. Uneven pattern of dopamine loss in the striatum of patients with idiopathic Parkinson's disease. Pathophysiologic and clinical implications. N Engl J Med 1988;318:876–880.
44. Langley J, Huddleston DE, Merritt M, et al. Diffusion tensor imaging of the substantia nigra in Parkinson's disease revisited. Hum Brain Mapp 2016;37:2547–2556.
45. Burciu RG, Ofori E, Archer DB, et al. Progression marker of Parkinson's disease: a 4-year multi-site imaging study. Brain J Neurol 2017;140:2183–2192.
46. Andrews JM. Striatonigral degeneration: clinical-pathological correlations and response to stereotaxic surgery. Arch Neurol 1970;23:319
47. Bannister R, Gibson W, Michaels L, Oppenheimer DR. Laryngeal abductor paralysis in multiple system atrophy: a report on three necropsied cases, with observations on the laryngeal muscles and the nuclei ambigui. Brain 1981;104:351–368. https://pubmed.ncbi.nlm.nih.gov/7237099/
48. Sung JH, Mastri A, Segal E. Pathology of Shy-Drager syndrome. J Neuropathol Exp Neurol 1979;38(4):353
49. Borit A, Rubinstein L, Urich H. The striatonigral degenerations: putaminal pigments and nosology. Brain 1975;98(1):101–112.
50. Rajput AH, Kazi KH, Rozdilsky B. Striatonigral degeneration response to levodopa therapy. J Neurol Sci 1972;16:331–341.

51. Dickson DW, Lin W, Liu W-K, Yen S-H. Multiple system atrophy: a sporadic synucleinopathy. Brain Pathol 1999;9:721–732.

52. Chougar L, Pyatigorskaya N, Degos B, Grabli D, Lehéricy S. The role of magnetic resonance imaging for the diagnosis of atypical parkinsonism. Front Neurol 2020;11:665

53. Pellecchia MT, Barone P, Vicidomini C, et al. Progression of striatal and extrastriatal degeneration in multiple system atrophy: a longitudinal diffusion-weighted MR study. Mov Disord 2011;26:1303–1309.

54. Tsukamoto K, Matsusue E, Kanasaki Y, et al. Significance of apparent diffusion coefficient measurement for the differential diagnosis of multiple system atrophy, progressive supranuclear palsy, and Parkinson's disease: evaluation by 3.0-T MR imaging. Neuroradiology 2012;54:947–955.

55. Meyer PT, Frings L, Rücker G, Hellwig S. 18F-FDG PET in parkinsonism: differential diagnosis and evaluation of cognitive impairment. J Nucl Med 2017;58:1888–1898.

56. Brooks DJ, Ibanez V, Sawle GV, et al. Differing patterns of striatal 18F-dopa uptake in Parkinson's disease, multiple system atrophy, and progressive supranuclear palsy. Ann Neurol 1990;28: 547–555.

57. Kim Y, Kim J-M, Kim J-W, et al. Dopamine transporter density is decreased in parkinsonian patients with a history of manganese exposure: what does it mean? Mov Disord 2002;17:568–575.

58. Ofori E, Krismer F, Burciu RG, et al. Free water improves detection of changes in the substantia nigra in parkinsonism: a multisite study. Mov Disord 2017;32:1457–1464.

59. Porrino LJ, Goldman-Rakic PS. Brainstem innervation of prefrontal and anterior cingulate cortex in the rhesus monkey revealed by retrograde transport of HRP. J Comp Neurol 1982;205:63–76.

60. Lehéricy S, Hartmann A, Lannuzel A, et al. Magnetic resonance imaging lesion pattern in Guadeloupean parkinsonism is distinct from progressive supranuclear palsy. Brain J Neurol. 2010;133: 2410–2425.

61. Braak H, Del Tredici K, Rüb U, de Vos RAI, Jansen Steur ENH, Braak E. Staging of brain pathology related to sporadic Parkinson's disease. Neurobiol Aging 2003;24:197–211.

62. Knudsen K, Fedorova TD, Hansen AK, et al. In-vivo staging of pathology in REM sleep behaviour disorder: a multimodality imaging case-control study. Lancet Neurol 2018;17:618–628.

63. Braak H, Braak E. Neuropathological stageing of Alzheimer-related changes. Acta Neuropathol (Berl) 1991;82:239–259.

64. Franzmeier N, Neitzel J, Rubinski A, et al. Functional brain architecture is associated with the rate of tau accumulation in Alzheimer's disease. Nat Commun 2020;11:347

65. Luk KC, Kehm V, Carroll J, et al. Pathological α-synuclein transmission initiates Parkinson-like neurodegeneration in non-transgenic mice. Science 2012;338:949–953.

66. Borghammer P. How does parkinson's disease begin? Perspectives on neuroanatomical pathways, prions, and histology. Mov Disord 2018;33:48–57.

67. Pandya S, Zeighami Y, Freeze B, et al. Predictive model of spread of Parkinson's pathology using network diffusion. Neuroimage 2019; 192:178–194.

68. Williams DR, Holton JL, Strand C, et al. Pathological tau burden and distribution distinguishes progressive supranuclear palsy-parkinsonism from Richardson's syndrome. Brain J Neurol 2007; 130:1566–1576.

69. Jellinger KA. A critical reappraisal of current staging of Lewy-related pathology in human brain. Acta Neuropathol (Berl) 2008;116:1–16.

70. Jellinger KA. Formation and development of Lewy pathology: a critical update. J Neurol 2009;256(suppl 3)):270–279.

71. Ogisu K, Kudo K, Sasaki M, et al. 3D neuromelanin-sensitive magnetic resonance imaging with semi-automated volume measurement of the substantia nigra pars compacta for diagnosis of Parkinson's disease. Neuroradiology 2013;55:719–724.

72. Liu XL, Yang LQ, Liu FT, et al. Short-echo-time magnitude image derived from quantitative susceptibility mapping could resemble neuromelanin-sensitive MRI image in substantia nigra. BMC Neurol 2020;20:262

73. Schwarz ST, Rittman T, Gontu V, Morgan PS, Bajaj N, Auer DP. T1-weighted MRI shows stage-dependent substantia nigra signal loss in Parkinson's disease. Mov Disord 2011;26:1633–1638.

Supporting Data

Additional Supporting Information may be found in the online version of this article at the publisher's web-site.